

Molecular dynamics simulation of a nanocluster obtained from the mining industry

Simulación mediante dinámica molecular de un nanocluster obtenido de la industria minera

Karen Isela Vargas-Rubio¹, Hiram Medrano- Roldán¹, Damián Reyes-Jáquez^{1*}

¹Unidad de Posgrado, Investigación y Desarrollo Tecnológico, Tecnológico Nacional de México - Instituto Tecnológico de Durango, Felipe Pescador 1830, Nueva Vizcaya, 34080, Durango, Dgo., México, damian.reyes@itdurango.edu.mx

*Autor de correspondencia

Abstract

A dynamic molecular simulation is a straightforward and logical research tool governed by Newton's movement equations. In this case, it is part of a new research line that explores the molecular interactions of a concentrate obtained from the mining industry (nanocluster). Mineragraphic and mineralogic analyses were performed, and 26 crystalline species were obtained and modeled, being chalcopyrite, pyrite, Cd-sulphide, quartz, and calcite the most representative structures due to their content. A geometry optimization applying the Quasi-Newton BFGS method was performed through the Materials Studio software version 8.0, obtaining the crystalline nanostructures. Finally, 95% of the structures were optimized, and more than 50% of these were validated based on X-ray diffraction (XRD) studies. Crystals that have not been validated have a different molecular weight and a different chemical composition and structure, affecting their crystallinity and X-ray diffraction patterns.

Keywords: Dynamic molecular simulation; crystal nanostructure; geometry optimization.

Resumen

La simulación dinámica molecular es una herramienta de investigación sencilla y lógica que se rige por las ecuaciones de movimiento de Newton. En este caso, es parte de una nueva línea de investigación que explora las interacciones moleculares de un concentrado obtenido de la industria minera (*nanocluster*). Se realizaron análisis minerográficos y mineralógicos, y se modelaron las 26 especies cristalinas obtenidas, siendo la calcopirita, pirita, sulfuro de cadmio, cuarzo y calcita las estructuras más representativas debido a su contenido. Se realizó una optimización geométrica aplicando el método Cuasi-Newton BFGS a través del *software* Materials Studio versión 8.0, obteniendo así las nanoestructuras cristalinas. Finalmente, se optimizaron el 95% de las estructuras y más del 50% se validaron con base a estudios de difracción de rayos X. Los cristales que no han sido validados tienen peso molecular, estructura y composición química diferente, lo cual afecta su cristalinidad y patrón de difracción de rayos X.

Palabras clave: Simulación dinámica molecular; nanoestructuras cristalinas; optimización geométrica.

Recibido: 29 de septiembre de 2020

Aceptado: 01 de marzo de 2021

Publicado: 05 de mayo de 2021

Como citar: Vargas-Rubio, K. V., Medrano- Roldán, H., & Reyes-Jáquez, D. (2021). Molecular dynamics simulation of a nanocluster obtained from the mining industry. *Acta Universitaria* 31, e3010. doi: http://doi.org/10.15174/au.2021.3010

Introduction

The continuous development of different research mechanisms, improved technologies, and tools in the study of various materials is carried out in different branches of science (Sharma *et al.*, 2019a; Tao & Dongwei, 2014). The impact of molecular dynamic simulations (MDS) in different branches of study has expanded dramatically in recent years. However, in the area of minerals extraction, MDS has not yet been widely used although it represents a great opportunity to solve problems within the mining area by allowing to achieve laboratory conditions that might be economically or physically restrictive in reality.

MDS can accurately predict how each atom in a molecular system will behave over time according to a general model of physics that governs interatomic interactions (Hollingsworth & Dror, 2018a). These simulations can analyze a wide variety of molecular processes such as conformational change, positioning of all atoms, in temporal resolution, prediction of new functional materials, and research of physical phenomena on a molecular level, among others (Lindahl, 2014; Sharma *et al.*, 2019a). MDS is a research tool which helps to understand chemical and biochemical processes, providing a dynamic dimension of structural data in addition to high precision atomic detail. There are mainly three areas of application for this type of study: 1) to build and analyze biomolecular structures, 2) to provide X-ray diffraction pattern, and 3) to explore the conformational space of biomolecules (Hollingsworth & Dror, 2018a; Lindahl, 2014; Sharma *et al.*, 2019b).

It is of utmost importance for this paper to be able to create each of the nanostructures, since they are the precursor structures of the nanocluster; however, there is very little information available regarding the structures, so it was necessary to validate them with a study of X-ray diffraction (XRD). Hence, the objective of this research was to simulate through molecular dynamics the crystalline structures of a concentrate obtained from the mining industry to create and validate a nanocluster.

Materials and Methods

Structure Preparation

From a mineragraphic analysis (QUEMSCAN PMA) (Avino Silver & Gold Mines, 2015) of a mineral concentrate obtained in Durango, Mexico, crystalline structures were identified and used as a starting point to model through the Visualizer Module of Materials Studio software version 8.0 (table 1).

Table 1. Crystal structures of mineral concentrate.

Name	Crystallization system	Space group	Lattice parameters (Å)
Argentite (Ag ₂ S)	Cubic	Im3m	a = 4.89
Pyrargyrite (Ag ₃ SbS ₃)	Trigonal	R3c	a = 11.047 c = 8.719
Stromeyerite (AgCuS)	Orthorhombic	Cmcm	a = 4.06 b = 6.66 c = 7.99
Chalcopyrite (CuFeS ₂)	Tetragonal	I-42D	a = 5.28 c = 10.41
Chalcocite (Cu ₂ S)	Monoclinic	P21/c	a = 11.881 b = 27.323 c = 13.491
Covellite (CuS)	Hexagonal	P63/mmc	a = 3.792 c = 16.344
Sphalerite (ZnS)	Cubic	F 4 3m	a = 5.406
Galena (PbS)	Cubic	Fm3m	a = 5.936
Bismuthinite (Bi ₂ S ₃)	Orthorhombic	Pbnm	a = 11.12 b = 11.25 c = 3.97

Bismuth	Trigonal	R3*m	a = 4.537 c = 11.838
Wittichenite (Cu ₃ BiS ₃)	Orthorhombic	P212121	a = 7.723 b = 10.395 c = 6.761
Cd - Sulphide (CdS)	Cubic	F 4 3 m	a = 5.825
Pyrite (FeS ₂)	Cubic	P a 3	a = 5.417
Arsenopyrite (FeAsS)	Monoclinic	P 2(1) / c	a = 5.74 b = 5.68 c = 5.79
Quartz (SiO ₂)	Trigonal	P 3 (2) 21	a = 4.913 b = 4.87 c = 5.405
K - Feldspars (KAlSi ₃ O ₈)	Monoclinic	C2/ m	a = 8.625 b = 12.996 c = 7.193
Chlorite (Mg, Fe) ₃ (Si, Al) ₄ O ₁₀ (OH) ₂ (Mg, Fe) ₃ (OH) ₆	Monoclinic	C2/m	a = 5.373 b = 9.306 c = 14.222
Anatase (TiO ₂)	Tetragonal	I4(1)/ amd	a = 3.793 c = 9.51
Calcite (CaCO ₃)	Trigonal	R3*c	a = 4.984 b = 4.934 c = 17.062
Rutile (TiO ₂)	Tetragonal	P4/mmm	a = 4.594 c = 2.958
Hematite (Fe ₂ O ₃)	Hexagonal	P6/m	a = 5.427 c = 5.427
Muscovite (KAl ₂ (AlSi ₅ O ₁₀)(OH) ₂)	Monoclinic	C2/m	a = 5.19 b = 9.03 c = 20.05
Acanth (Ag ₂ S)	Monoclinic	P21/n	a = 4.229 b = 6.931 c = 7.862
Stephanite (Ag ₅ SbS ₄)	Orthorhombic	Cmcm21	a = 7.793 b = 12.295 c = 8.506
Magnetite (Fe ²⁺ Fe ₂ ³⁺ O ₄)	Cubic	Fd3m	a = 8.391
Matildite (AgBiS ₂)	Hexagonal	P3*m1	a = 8.12 c = 19.02

Source: Authors' own elaboration.

Structure Optimization

Each structure was optimized according to an energy evaluation and conformational adjustment. Structural parameters were obtained by moving the constituent atoms to positions where the energy was minimal. This procedure was carried out using the CASTEP module by performing the Quasi-Newton BFGS method (Li & Fukushima, 2001; Pfrommer *et al.*, 1997; Zhou, 2020). This method accumulates information about enthalpy in the inverse of the Hess matrix, once the coordinates of the configuration space are defined. The crystalline structure is delimited by the matrix of lattice vectors $h = \{a, b, c\}$ and the coordinates $s_i = 1 \dots N$, relative to h of the N atoms in the unit cell, which has a volume of $\Omega = \det(h)$. Conveniently, strain tensor ϵ is chosen in exchange for the lattice vectors and is related to the reference configuration h_0 in h , as observed in equation 1.

$$h = (1 + \epsilon)h_0 \quad (1)$$

A point in configuration space by the column vector X and its deformation components, which is the negative of the derivative of the enthalpy H for X , is given by equation 2, also known as *force vector*.

$$F = - \left. \frac{\partial H}{\partial x} \right|_{p'} \quad (2)$$

Results

Structure Preparation

The structural information of the crystals found in the mineral concentrate is presented in table 1. All structures were created from their base structure. Representative examples are shown in figure 1.

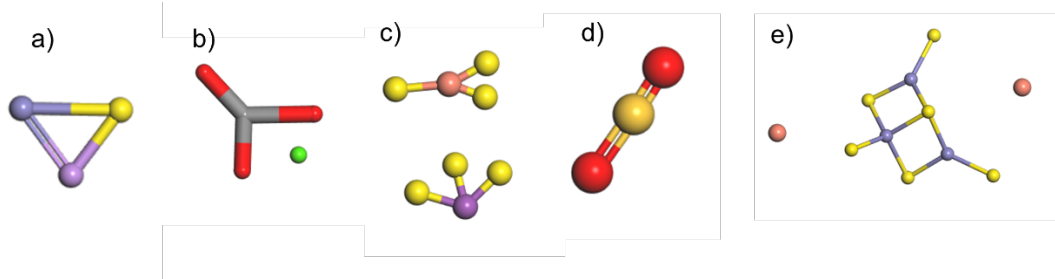


Figure 1. Base structures of a) Arsenopyrite, b) Calcite, c) Wittichenite d) Quartz, e) Chalcopyrite.
Source: Authors' own elaboration.

Structure Optimization

From the CASTEP module, the universal force field was chosen because it allows to analyze all metallic materials (BIOVIA, 2014c). Optimization of each structure was carried out using the quasi-Newton BFGS iterative method, in which, with each iteration, a value for energy is obtained. Figure 2 shows the energy optimization lines of the different crystalline structures.

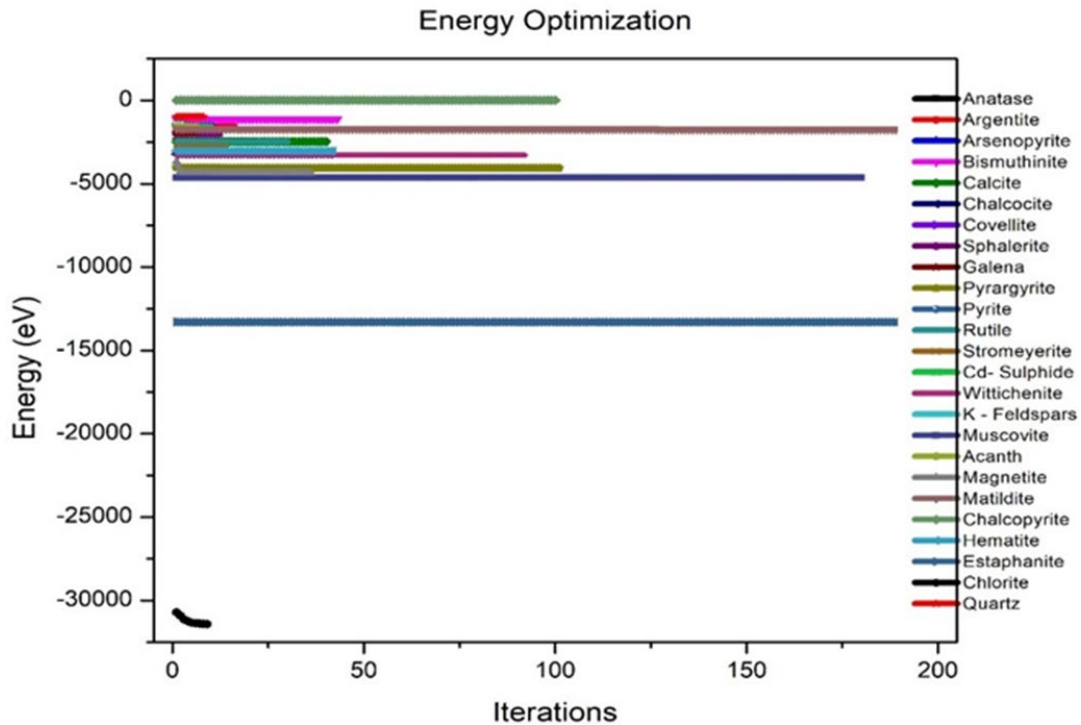


Figura 2. Optimización de todas las estructuras cristalinas simuladas.
Source: Authors' own elaboration.

Crystal Creation

Each crystal was created according to the specific lattice parameters, as well as the space group (BIOVIA, 2014a). For instance, arsenopyrite crystallizes in a monoclinic system in a space group $P 2(1)/c$, and it is composed of 46.01% arsenic, 34.30% iron, and 19.69% sulfur (figure 3a). Calcite is a mineral of calcium carbonate whose crystallization system is trigonal and its space group is $R\bar{3}c$, which is made up of 40.04% calcium and the rest is carbonate (figure 3b). Wittichenite is a very rare mineral that crystallizes in an orthorhombic system; its space group is $P2(1)2(1)2(1)$; and it is composed of sulfur, copper, and bismuth in 19.40%, 38.45%, and 42.15% respectively (figure 3c). Quartz is one of the best-known minerals on earth. It is composed of 46.74% silicon and the rest is oxygen, it crystallizes in a trigonal system and its space group is $P 3(2) 21$; its structure can be seen in figure 3d. Chalcopyrite, with a tetragonal crystallization system and an $I-42D$ space group, is composed in equal parts of copper and sulfur (34.78%) and the rest is iron (Cambridge Crystallographic Data Center [CCDC], 2020; Crystallography Open Database, 2020; Mineralogical Society of America [Minsocam], 2017) (figure 3e).

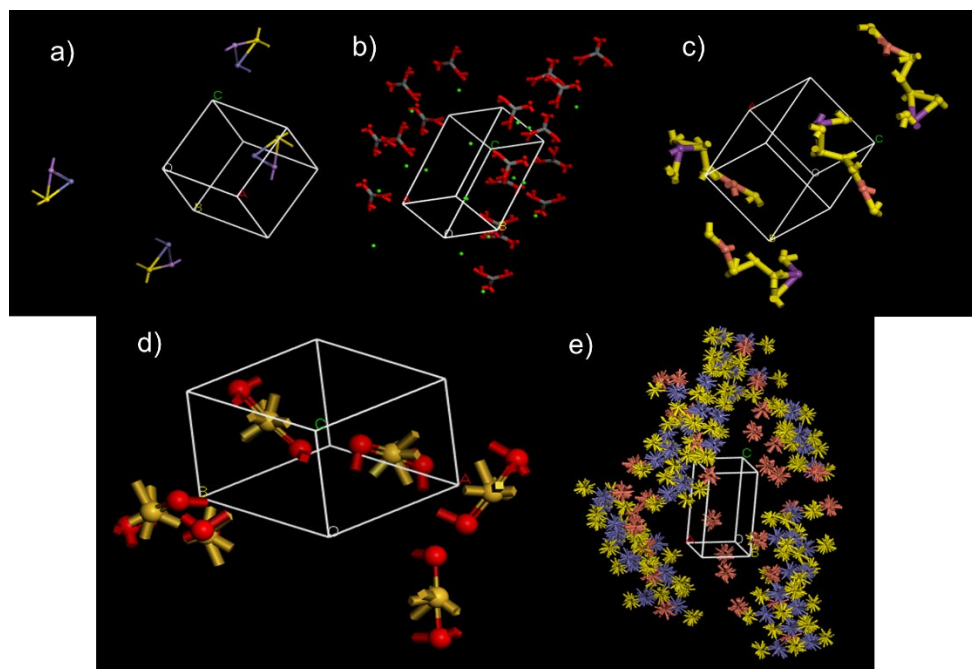


Figure 3. Examples of crystalline structures created in Materials Studio a) Arsenopyrite, b) Calcite, c) Wittichenite, d) Quartz, and, e) Chalcopyrite.

Source: Authors' own elaboration.

Validation of Crystalline Structures

The unit cell size and orientation of the crystal determine the position at which the diffraction patterns can be measured at the appropriate wavelength. The analysis of the positions of the diffraction peaks produces the unit cell size and its orientation (BIOVIA, 2014b); for this reason, to validate each one of the structures that were modeled in the simulator, lattice parameters and space groups were compared against those obtained from the XRD study (table 2). Not all crystals that were simulated appeared in the diffraction study; therefore, only the results of those that appeared in the study are shown.

Table 2. Validation of crystalline structures.

Crystal	XDR		SOFTWARE	
	Lattice parameters (Å)	Space group	Lattice parameters (Å)	Space group
Rutile	a = 10.4748	I213	a = 4.594 c = 2.958	P4/mmm
Arsenopyrite	a = 5.6007 b = 5.6155 c = 5.7246	P 2(1) / c	a = 5.74 b = 5.68 c = 5.79	P 2(1) / c
Bismuthinite	a = 11.281 b = 11.241 c = 3.935	Pnma	a = 11.12 b = 11.25 c = 3.97	Pbnm
Calcite	a = 5.405 b = 5.405 c = 19.68	R3*c	a = 4.984 b = 4.934 c = 17.062	R3*c
Chalcocite	a = 27.323 b = 13.491 c = 11.881	Fm-3m	a = 11.881 b = 27.323 c = 13.491	P21/c
Covellite	a = 3.792 c = 16.344	P63/mmc	a = 3.792 c = 16.344	P63/mmc
Sphalerite	a = 3 b = 3 c = 61	P3m1	a = 5.406	F 4*3m
Galena	a = 6.970 b = 5.209 c = 7.175	Pma2	a = 5.936	Fm3m
Pyrargyrite	a = 8.14 b = 8.07 c = 8.64	P -1	a = 11.047 c = 8.719	R3c
Pyrite	a = 5.4098	P a 3	a = 5.417 b = 5.424 c = 3.387	P a 3
Stromeyerite	a = 4 b = 6 c = 8	Cmcm	a = 4.06 b = 6.66 c = 7.99	Cmcm
Cd - Sulphide	a = 5.4027	F 4 3 m	a = 5.825	F 4 3 m
Wittichenite	a = 7 b = 11 c = 7	P212121	a = 7.723 b = 10.395 c = 6.761	P212121
Chalcopyrite	a = 5.2739 c = 10.393	I-42D	a = 5.28 c = 10.41	I-42D
K - Feldspars	a = 9.14 b = 9.14 c = 2.94	I4/m	a = 8.625 b = 12.996 c = 7.193	C2/ m
Acanth	a = 3.88 b = 5.89 c = 8.13	P21/n	a = 4.229 b = 6.931 c = 7.862	P21/n
Magnetite	a = 9.17 b = 7.982 c = 2.790	Bbmm	a = 8.391	Fd3m
Matildite	a = 13.01 b = 4.488 c = 16.940	C12/m1	a = 8.12 c = 19.02	P3*m1
Chlorite	a = 5.1 b = 7.8 c = 14.29	C2/m	a = 5.373 b = 9.306 c = 14.222	C2/m
Quartz	a = 4.905 b = 4.905 c = 5.379	P 3 (2) 21	a = 4.913 b = 4.87 c = 5.405	P 3 (2) 21
Bismuth	a = 8.6 c = 4.2	I4/mcmm	a = 4.537 c = 11.838	R3*m

Source: Authors' own elaboration.

Results shown in table 2 indicate that more than 50% of the crystals that appeared in the XRD study agree with the values used for the simulation. Furthermore, the lack of concordance might occur because of the discrepancy of their chemical composition, resulting in a mismatch of space groups, in that several crystals depend on pressure and temperature to define the previously mentioned parameters, which may present variations.

X-ray Diffraction Study

Minerals are crystalline and the spatial distribution of their components is arranged as structured networks (Consejo Superior de Investigaciones Científicas [CSIC], 2020; Servicio Geológico Mexicano [SGM], 2010); hence, XRD studies can also be used to obtain the diffraction pattern of the sample (figure 4) quantitative analyzes.

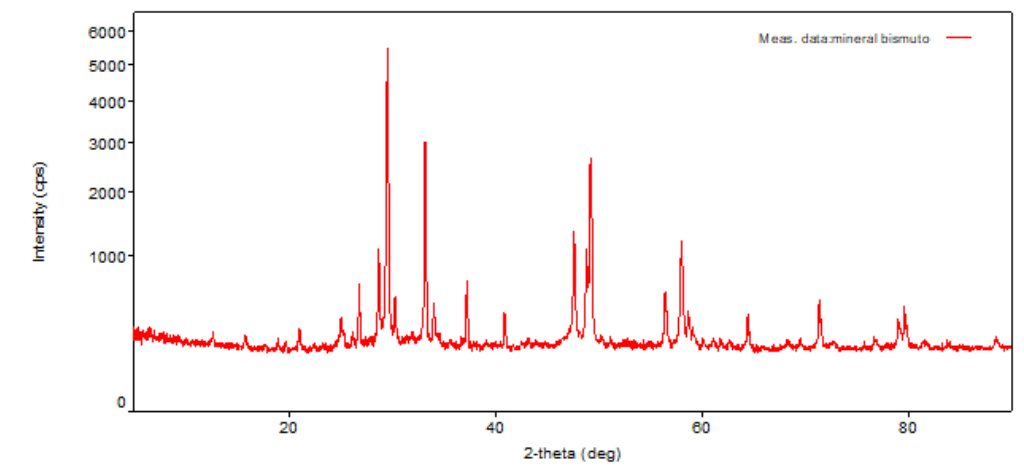


Figure 4. XDR pattern obtained experimentally
Source: Authors' own elaboration.

Subsequently, the simulation of the diffraction patterns of each crystal structure that appeared in the study was performed. This procedure was carried out using the REFLEX module of the same software (BIOVIA, 2014d). The obtained results can be seen in figure 5. However, it is a considerably different pattern from the one observed in figure 4, this may be because in the simulation each crystal is individually analyzed, whereas in the study carried out experimentally the sample of the mining concentrate contains all its components at once.

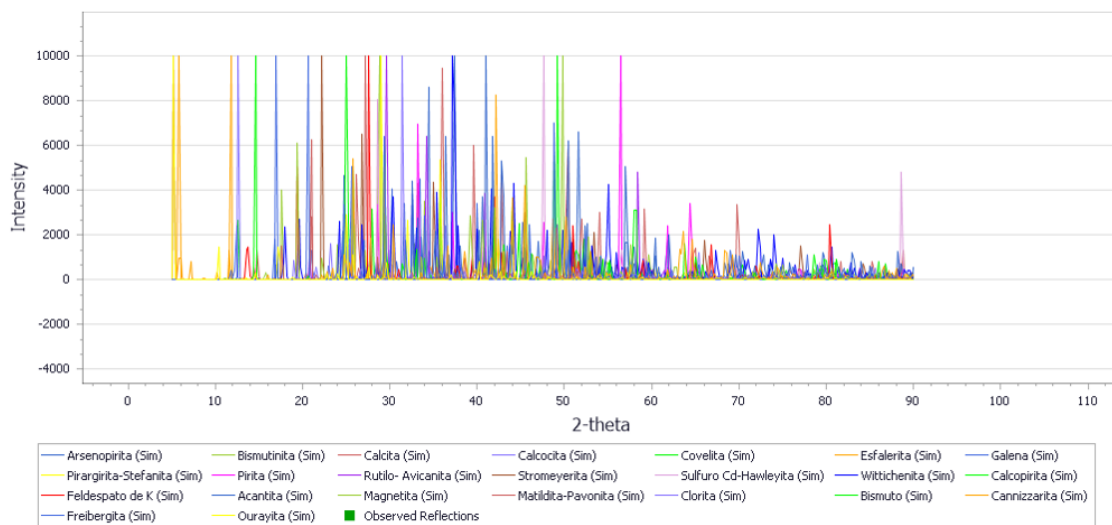


Figure 5. XDR patterns of simulated crystal structures
Source: Authors' own elaboration.

To analyze the similarity of the XRD patterns, further research is required for each pure crystal to fully compare figures 4 and 5.

Discussion

The nanocrystals were optimized using the CASTEP module, because it is a state-of-the-art quantum mechanics-based program, designed specifically for solid-state materials science (Clark *et al.*, 2005). In this module, as mentioned before, the quasi-Newton method was developed with a BFGS fit, since it is the only iterative method for optimizing crystal structures.

Each structure created was validated to have the most probable structure close to reality, by making a comparative study between the x-ray diffraction pattern that could be simulated with the pattern obtained from an experimental study.

The creation, optimization, and subsequent validation of each crystal structure lead to the formation of a nanocluster with characteristics similar to a mineral sample that can be widely used for exploratory research, unlike a more orthodox experimental research which might have limiting factors such as the expense of reagents, time consumption, and some physical processing conditions that could be difficult to achieve at laboratory scale.

Conclusions

All the crystalline structures present in the mineragraphic analysis were simulated in the visualizer module, and the optimization of the geometry of 95% of the structures created using the Quasi-Newton BFGS method in the CASTEP module was achieved. On the other hand, all crystals of the optimized structures were created, each one with the corresponding parameters and angles, and 72.5% of the structures were validated by comparing the X-ray diffraction pattern against the simulated pattern. Finally, once the simulation is validated, the metal recovery process can be made more efficient by avoiding time investment in experiments and the use of reagents.

References

- Avino Silver & Gold Mines. (2015). *Mineralogical study on a copper concentrate sample bureau veritas commodities Canada Ltd. Avino*. doi: <https://doi.org/10.13140/RG.2.2.20442.47049>
- BIOVIA. (2014a). *Building and rebuilding crystals*. doi: <https://doi.org/10.13140/RG.2.2.15409.30563>
- BIOVIA. (2014b). *Diffraction from a single crystal. Theory in Reflex*.
Doi: <https://doi.org/10.13140/RG.2.2.24636.77443>
- BIOVIA. (2014c). *Materials studio*. doi: <https://doi.org/10.13140/RG.2.2.36380.82565>
- BIOVIA. (2014d). *Diffraction from powder samples*. doi: <https://doi.org/10.13140/RG.2.2.10795.57129>
- Cambridge Crystallographic Data Center (CCDC). (2020). [*Crystallographic classification*]. CCDC.
<https://www.ccdc.cam.ac.uk/>
- Clark, S. J., Segall, M. D., Pickard, C. J., Hasnip, P. J., Probert, M. I., Refson, K., & Payne, M. C. (2005). First principles methods using CASTEP. *Zeitschrift Fuer Kristallographie*, 220(5-6), 567-570.
doi: <https://doi.org/10.1524/zkri.220.5.567.65075>
- Consejo Superior de Investigaciones Científicas (CSIC). (2020). *Cristalografía*. CSIC.
<https://www.xtal.iqfr.csic.es/Cristalografia/>

- Crystallography Open Database. (2020). [Open-access collection of crystal structures of organic, inorganic, metal-organics compounds and minerals, excluding biopolymers]. Crystallography. <http://www.crystallography.net/cod/>
- Hollingsworth, S. A., & Dror, R. O. (2018a). Molecular dynamics simulation for all. *Neuron*, 99(6), 1129–1143. doi: <https://doi.org/10.1016/j.neuron.2018.08.011>
- Li, D., & Fukushima, M. (2001). A modified BFGS method and its global convergence in nonconvex minimization. *Journal of Computational and Applied Mathematics*, 129(1-2), 15–35. doi: [https://doi.org/10.1016/S0377-0427\(00\)00540-9](https://doi.org/10.1016/S0377-0427(00)00540-9)
- Lindahl, E. (2014). Molecular dynamics simulations. *Molecular Modeling of Proteins*, 1215, 3–26. doi: https://doi.org/10.1007/978-1-4939-1465-4_1
- Pfrommer, B. G., Cote, M., Louie, S. G., & Cohen, M. L. (1997). Relaxation of crystals with the quasi-Newton method. *Journal of Computational Physics*, 131(1), 233–240. doi: <https://doi.org/10.1006/jcph.1996.5612>
- Mineralogical Society of America (Minsocam). (2017). *American mineralogist*. Minsocam. <http://www.minsocam.org/msa/AmMin/AmMineral.html>
- Servicio Geológico Mexicano (SGM). (2010). *Difracción de rayos X*. SGM. <https://www.sgm.gob.mx/Web/MuseoVirtual/Minerales/Difraccion-de-rayos-X.html>
- Sharma, S., Kumar, P., & Chandra, R. (2019a). Introduction to molecular dynamics. In S. Sharma (ed.), *Molecular dynamics simulation of nanocomposites using BIOVIA materials studio, Lammmps and Gromacs* (pp. 1-38). Elsevier Inc. doi: <https://doi.org/10.1016/B978-0-12-816954-4.00001-2>
- Sharma, S., Kumar, P., & Chandra, R. (2019b). Overview of BIOVIA materials studio. In S. Sharma (ed.), *Molecular Dynamics Simulation of Nanocomposites Using BIOVIA Materials Studio, Lammmps and Gromacs* (pp. 39-100). Elsevier Inc. doi: <https://doi.org/10.1016/B978-0-12-816954-4.00002-4>
- Tao, H., & Dongwei, L. (2014). Presentation on mechanisms and applications of chalcopyrite and pyrite bioleaching in biohydrometallurgy – a presentation. *Biotechnology Reports*, 4, 107–119. doi: <https://doi.org/10.1016/j.btre.2014.09.003>
- Zhou, W. (2020). A modified BFGS type quasi-Newton method with line search for symmetric nonlinear equations problems. *Journal of Computational and Applied Mathematics*, 367. doi: <https://doi.org/10.1016/j.cam.2019.112454>